HHS Public Access

Author manuscript

Oncogene. Author manuscript; available in PMC 2010 July 21.

Published in final edited form as:

Oncogene. 2010 January 21; 29(3): 368–379. doi:10.1038/onc.2009.360.

Inhibition of Eyes Absent Homolog 4 expression induces malignant peripheral nerve sheath tumor necrosis

Shyra J. Miller[1,*], **Zheng D. Lan**[1,*], **Atira Hardiman**[1], **Jianqiang Wu**[1], **Jennifer J. Kordich**[1], **Deanna M. Patmore**[1], **Rashmi S. Hegde**[2], **Timothy P. Cripe**[3], **Jose A. Cancelas**[1], **Margaret H. Collins**[4], and **Nancy Ratner**[1]

[1]Division of Experimental Hematology and Cancer Biology, Cincinnati Children's Hospital Research Foundation, University of Cincinnati College of Medicine, Cincinnati, Ohio 45229, USA.

[2]Division of Developmental Biology, Cincinnati Children's Hospital Research Foundation, University of Cincinnati College of Medicine, Cincinnati, Ohio 45229, USA.

[3]Division of Hematology/Oncology, Cincinnati Children's Hospital Research Foundation, University of Cincinnati College of Medicine, Cincinnati, Ohio 45229, USA.

[4]Division of Pathology, Cincinnati Children's Hospital Research Foundation, University of Cincinnati College of Medicine, Cincinnati, Ohio 45229, USA.

Abstract

Malignant peripheral nerve sheath tumors (MPNSTs) are aggressive sarcomas without effective therapeutics. Bioinformatics was used to identify potential therapeutic targets. *Paired Box (PAX)*, *Eyes Absent* (*EYA*), *Dachsund* (*DACH*), and *Sine Oculis* (*SIX*) genes, which form a regulatory interactive network in drosophila, were found to be dysregulated in human MPNST cell lines and solid tumors. We identified a decrease in *DACH1* expression, and increases in expression of *PAX6*, *EYA1*, *EYA2*, *EYA4*, and *SIX1- 4*. Consistent with the observation that half of MPNSTs develop in neurofibromatosis type 1 patients, subsequent to *NF1* mutation, we found that exogenous expression of the NF1-GAP related domain (GRD) normalized *DACH1* expression. *EYA4* mRNA was elevated more than 100-fold as estimated by quantitative real time PCR in most MPSNT cell lines. *In vitro*, suppression of *EYA4* expression using shRNA reduced cell adhesion and migration and caused cellular necrosis without affecting cell proliferation or apoptotic cell death. MPNST cells expressing sh-EYA4 either failed to form tumors in nude mice or formed very small tumors, with extensive necrosis but similar levels of proliferation and apoptosis as control cells. Our findings identify a role for EYA4 and possibly interacting SIX and DACH proteins in MPNSTs and suggest the EYA4 pathway as a rational therapeutic target.

Corresponding author: Nancy Ratner, Ph.D., Division of Experimental Hematology and Cancer Biology, Cincinnati Children's Hospital Research Foundation, 3333 Burnet Avenue, MLC 7013, Cincinnati, OH 45229-3039, USA, Phone: (513) 636-9469 | Fax: (513) 636-3549, nancy.ratner@cchmc.org.

*These authors contributed equally to this work.

Keywords

EYA4; MPNST; NF1; DACH1; SOX9; Ras

Introduction

Malignant peripheral nerve sheath tumors (MPNSTs) are highly aggressive soft tissue sarcomas with a poor prognosis. Half of MPNST cases arise in individuals with Neurofibromatosis type 1 (NF1), an autosomal dominant disorder affecting approximately 1 in 3500 individuals worldwide (Friedman *et al.* 1997; Rasmussen *et al.* 2000). While sporadic MPNSTs develop in the general population at the low incidence of 0.0001%, the lifetime risk of an NF1 patient developing MPNST is as high as 8–13% (Evans *et al.* 2002). There is evidence suggesting that cells within plexiform neurofibromas, benign tumors found in approximately 30% of NF1 patients, undergo malignant transformation and give rise to MPNST (Leroy *et al.* 2001; Ferner *et al.* 2002; Carroll *et al.* 2008). MPNST remains a major source of mortality for NF1 patients, because there is currently no effective therapy. Conventional radiation and chemotherapy are generally unsuccessful in controlling MPNST growth, especially in NF1 patients. Although early detection and excision of the tumor improve survival, complete resection is not always feasible and local recurrence is common (Carli *et al.* 2005). Metastasis to the lung, liver, and brain is also observed (Ferner *et al.* 2002). While the clinical course of NF1-associated MPNSTs is considerably worse than that of sporadic MPNSTs, their gene expression profiling is indistinguishable (Holtkamp *et al.* 2004; Watson *et al.* 2004; Miller *et al.* 2006).

A major pathway implicated in MPNST formation is the NF1-Ras pathway. The *NF1* gene product, neurofibromin, is one of a family of GTPase activating proteins (GAPs) that accelerates the hydrolysis of active Ras-GTP to inactive Ras-GDP (McCormick 1995). Single missense mutations in the GAP-related domain (GRD) of *NF1* have been detected in patients (Klose *et al.* 1998). Furthermore, MPNST cell lines and tumors have elevated basal Ras-GTP (Basu *et al.* 1992; DeClue *et al.* 1992; Kim *et al.* 1995; Sherman *et al.* 2000). Replacing the NF1-GRD rescued the cardiovascular defect responsible for embryonic lethality in Nf1-deficient mice but did not rescue abnormalities in neural crest development (Ismat *et al.* 2006), although several lines of evidence support the neural crest origin of NF1-associated MPNSTs (reviewed in Carroll *et al.* 2008; Miller and Jessen *et al.* 2009; Vogel et al., 1999), suggesting involvement of additional or alternative molecular pathways in NF1 tumorigenesis.

To identify dysregulated molecular pathways in MPNSTs that might guide novel therapeutic strategies, we recently conducted global gene expression analysis of NF1-associated tumors and tumor-derived Schwann cells, including sporadic and NF1-derived MPNSTs, on the whole-genome Affymetrix platform (Miller and Jessen *et al.* 2009). The mRNA encoding the SOX9 transcription factor was over-expressed in benign MPNST precursor lesions (neurofibroma), and expression of *SOX9* was further elevated in MPNSTs. Computational promoter analysis identified *EYA4*, a gene highly expressed in MPNSTs, as a potential transcriptional target of SOX9. Supporting the *in silico* analysis, inhibition of *SOX9*

expression using shRNA in MPNST cells reduced *EYA4* expression levels, and exogenous expression of *SOX9* in normal human Schwann cells and neurofibroma cells increased *EYA4* expression levels.

The transcriptional network involving members of the *EYA*, *SIX*, *DACH*, and *PAX* gene families was originally characterized in fly eye development and is commonly referred to as the retinal determination (RD) pathway (Silver *et al.* 2005). While the epistatic relationships among the ey-so-eya-dac genes in flies is well characterized, the expression relationships among the vertebrate Pax-Six-Eya-Dach genes differ based on tissue types and stages of development. The SIX proteins are DNA-binding transcription factors, which variously activate (Xu *et al.* 1996) or repress (Kobayashi *et al.* 2001; Zhu *et al.* 2002) transcription. The DACH proteins can also activate (Ikeda *et al.* 2002) or repress (Wu *et al.* 2006; Wu *et al.* 2009) transcription in a context-dependent fashion. EYA proteins are both transcriptional activators (Xu *et al.* 1996) and tyrosine phosphatases (Rayapureddi *et al.* 2003; Tootle *et al.* 2003) and have recently been shown to dephosphorylate H2AX, promoting repair and cell survival in the response to DNA damage (Cook *et al.* 2009). EYA proteins (EYA1 - 4) are normally expressed early in development (Xu *et al.* 1996; Abdelhak *et al.* 1997; Borsani *et al.* 1999) and promote stem cell survival (Li *et al.* 2003). This is relevant, because mouse and human MPNST cells have characteristics of neural crest stem cells (Josephson *et al.* 1998; Vogel *et al.* 1999; Miller and Jessen *et al.* 2009).

Individual members of the RD pathway have been implicated in tumorigenesis (Christensen *et al.* 2008). Expression of several *PAX* family members has been associated with cancer cell line survival (Muratovska *et al.* 2003). Downregulation of *DACH1* expression has been observed in breast (Wu *et al.* 2006) and prostate cancer (Wu *et al.* 2006; Wu *et al.* 2009). Upregulation of *SIX1* expression has been observed in a variety of cancers (Reichenberger *et al.* 2005; Ng *et al.* 2006; Behbakht *et al.* 2007; Kroemer *et al.* 2009), and overexpression of SIX1 is sufficient for malignant transformation of mammary cells (Coletta *et al.* 2008). Overexpression of *EYA2* has been shown to promote ovarian tumor growth (Ramdas *et al.* 2001). Here, we describe the dysregulation of a transcriptional network consisting of the *EYA*, *SIX*, *DACH* and *PAX* genes in MPNSTs and provide evidence supporting a role for EYA4 in MPNST survival and tumorigenesis.

Materials and Methods

Microarray analyses

Collection of samples, RNA isolation, probe generation, Affymetrix HU133 Plus 2.0 microarray hybridization, and normalization of data was conducted as described for differential gene expression in neurofibroma and MPNST samples relative to normal human Schwann cells (Miller and Jessen et al., 2009). Using Genespring GX v7.3.1 (Agilent Technologies), hierarchical cluster analysis was conducted for all family members of the RD transcriptional network, and analysis of variance (ANOVA) with a Benjamini and Hochberg false discovery rate correction (FDR = 0.01) was used to determine statistically significant changes in gene expression between normal human Schwann cells, neurofibroma samples, and MPNST samples. For comparison of MPNST cells infected with adenovirus, gene expression was normalized to the average gene expression amongst three independent

normal human Schwann cell samples. Statistical analyses (ANOVA; FDR = 0.001) were used to identify significant gene expression changes between uninfected MPNST cells, MPNST cells infected with control (GFP) virus, and MPNST cells infected with NF1-GRD virus.

Cell Culture and Tissue Samples

Normal human Schwann cells (NHSCs) were cultured from trauma victims (Casella *et al.* 1996) and Schwann cells were cultured from dermal neurofibromas as described (Serra *et al.* 2000). MPNST cell lines were cultured as described (Miller *et al.* 2006; Mahller *et al.* 2007). NHSC = normal human Schwann cells; dNFSC = dermal neurofibroma Schwann cells; dNF = primary dermal neurofibromas; pNFSC = plexiforma neurofibroma Schwann cells; pNF = plexiform neurofibromas; MPNST = malignant peripheral nerve sheath tumor; MPNST cell lines include: STS26T, ST8814, S462, S520, T265, 908-8, 88-3, and YST1.

Adenoviral infection

The NF1-GRD adenovirus was constructed by inserting a ~1.1kb Xba/HindIII fragment containing the coding sequence for the human NF1-GRD isoform I (GenBank NM_000267; (Viskochil *et al.* 1992) and a 5'-HA tag into the pAdTrack vector (He *et al.* 1998). The resulting vector, pAdTrack-NF1-GRD-HA, was linearized with PmeI and transformed into BJ5183 cells containing the pAdEasy vector. Recombinants were screened by restriction digestion, sequence-verified, and then transformed into DH5α cells for amplification. Amplified clones were verified by HA expression and ability to reduce Ras activity (see below). For microarray and QRT-PCR experiments, MPNST cells were infected with an adenoviral construct expressing the NF1-GRD or GFP, in triplicate, with cesium-purified adenovirus for 2 hours in serum-free medium at 200pfu/cell. Viruses were washed away and cells cultured in normal medium for another 30 hours, then RNA isolated as above was isolated for analysis of gene expression as described (Miller and Jessen *et al.* 2009).

Lentiviral infection

For lentiviral shRNA infection, MPNST cells at 70 – 90% confluence were infected with lentiviral particles containing shRNAs targeting EYA4 (Open Biosystems; TRC library) or GFP (Addgene). The CCHMC Viral Vector Core produced virus using a 4-plasmid packaging system (http://www.cincinnatichildrens.org/research/div/exp-hematology/translational/vpf/vvc/default.htm). Lentiviral particles were incubated with MPNST cells (MOI ~ 10) in the presence of polybrene (8 μg/mL; Sigma) for 24 hours followed by selection in puromycin at a concentration (2 μg/mL) that killed uninfected cells within three days.

Quantitative real time PCR (QRT)-PCR

Total RNA was isolated from cells using the RNeasy kit (Qiagen) and used as a template for cDNA synthesis (Invitrogen Superscript II) and QRT-PCR (ABI 7500 Sequence Detection System) as described (Miller *et al.* 2006).

Western Analysis

Cell lysates were created and Western blotting conducted as described (Miller *et al.* 2006), membranes were probed with anti-EYA4 antibodies (Santa Cruz Biotechnology, Inc.; EYA4 (E-20): sc-15107), then, stripped and re-probed with anti-β-actin antibodies (Cell Signaling Technology, Inc. #4967) as a loading control. Signals were detected using horseradish peroxidase-conjugated secondary antibodies (BioRad; Hercules, CA) and the ECL Plus developing system (Amersham Biosciences; Piscataway, NJ). ImageJ 1.33u software (http://rsb.info.nih.gov/ij/) was used to quantify EYA4 from scanned autoradiographs.

Ras activation assay

Ras activity was measured in MPNST cells as described (Mahller *et al.* 2006). MPNST cell lines were infected with the NF1-GRD adenovirus or a vector encoding green fluorescent protein. Two days later lysates were prepared and blotted directly for total canonical Ras proteins (H,N,K-Ras), active ERK, or active MEK. Ras-GTP was evaluated by centrifuging beads conjugated with GST-Raf-RBD from cell lysates, and probing by Western blots (Ras Activation Assay; Upstate Biotechnology).

Bromodeoxyuridine (BrdU) Incorporation

Twenty-four hours post-plating 3×10^4 MPNST cells onto glass coverslips, cells were labeled for one hour with BrdU labeling reagent, fixed in ethanol, and incubated with anti-BrdU antibodies followed by detection with fluorescein-conjugated secondary antibodies according to the manufacturer's protocol (5-Bromo-2'-deoxy-uridine Labeling and Detection Kit II; Roche Applied Science). All cell nuclei were labeled with propidium iodide (PI; 50 μg/mL). Total number of cells (PI+) and number of BrdU positive cells were counted in five fields per sample and averaged.

Detection of apoptotic cells

MPNST cells were plated in quadruplicate wells (2×10^4 cells/well) of LabTek chamber slides (Nalge-Nunce International), then infected with shEYA4 or shGFP lentiviral particles. After 3 days in the presence or absence of puromycin, cells were fixed for detection of DNA damage in apoptotic cells (Apo ssDNA kit; Cell Technology, Inc.). Briefly, DNA was denatured, and single-stranded DNA (ssDNA) was detected with a primary anti-ssDNA antibody, followed by tetramethylrhodamine isothiocyanate (**TRITC**)-conjugated secondary antibodies. Five random fields in triplicate wells were counted, and TRITC-positive apoptotic cells were expressed as a percentage of total cells visualized by bisbenzimide staining of nuclei.

Detection of necrotic cells

Live MPNST cells were incubated with propidium iodide (PI; Sigma; 50 μg/mL) for 2 hours at room temperature, 24 hours after plating at a density of 50,000 cells per well in 35mm dishes. Cells were photographed in 7 randomly chosen fields per dish, in each of 2 dishes per condition. PI-positive cells (necrotic cells) were expressed as a percentage of total cells.

Migration assay

The migratory response of MPNST cells was measured using a modified Boyden chamber assay as described (Miller *et al.* 2006). MPNST cells (4×10^4) expressing shGFP or shEYA4 were plated in serum-free DMEM on the upper chamber of a transwell with 8 μm pores (Costar); The lower chamber contained 800 μl DMEM plus serum. Cells were incubated for 16 h at 37°C in 10% CO_2. Nonmigrating cells were removed from the upper surface of the membrane with cotton swabs. Membranes were stained with bisbenzimide and mounted onto glass slides. Migration was quantified by counting cells in four fields. Each condition was performed in triplicate, and the number of migrated cells was normalized to the total number of cells on an unscraped filter to validate the total number of cells plated. Data shown are representative of three independent experiments; values presented are the mean±s.d. Statistical significance was determined by *t*-test using Microsoft Excel software.

Mouse xenograft

Mouse xenografts of MPNST cells were conducted as described (Mahller *et al.* 2008). 1.2 $\times 10^6$ one million S462TY MPNST cells expressing shControl (n=10), shEYA4.3 (n=10), shEYA4.5(n=10), or shEYA4.7 (n=10) were injected subcutaneously into 6-to 8-week-old female athymic nude (nu/nu) mice (Harlan, Indianapolis, IN). Left and right flanks were injected with control or shEYA cells in each animal. In accordance with CCHMC rodent tumor guidelines, tumors may not exceed 10% of body weight. Tumors formed in shControl cells in approximately 30 days, reaching ~2000 mm^3 in approximately 60 days. Therefore, 59 days post-injection, we measured tumor volume and euthanized all shControl mice and shEYA mice. Tumors were dissected and submitted to the CCHMC Pathology Lab for histological characterization, including H&E staining, Mib-1 detection of proliferating cells, TUNEL, and detection of blood vessels using anti-CD31.

Adhesion assay

MPNST cells expressing shGFP or shEYA4 (10^4 cells per well on LabTek slides) were plated and incubated in standard growth conditions for 2 hours. The wells were gently washed with PBS to remove non-adherent cells, and remaining adherent cells were counted. Adhesion was quantified by counting cells in six fields per well.

FACS analysis

Approximately 100,000 MPNST-shControl, MPNST-shEYA4.3, or MPNST-shEYA4.7 cells were fixed in 0.5% paraformaldehyde, permeabilized 0.1% Triton X100 and incubated for one hour at 4°C in PBS constaining RNAseA (2 mg/mL) and propidium iodide (50 μg/mL). Flow cytometry analysis was performed in a FACSCanto (Becton Dickinson, San Jose, CA). Analysis of forward scatter (FSC) and side scatter (SSC) in linear amplification was performed along cell cycle analysis. Identification of the A_o (apoptotic), G_o/G, S, and G2/M peaks were performed by ModFit (Verity, Topsham, ME) analysis.

Results

Expression of genes comprising the Retinal Determination pathway is dysregulated in MPNST

Global gene expression profiling in NF1-associated tumors and Schwann cells revealed a cluster of genes significantly over-expressed in MPNSTs relative to neurofibromas and normal Schwann cells (Miller and Jessen *et al.* 2009). A striking observation within this cluster is an up-regulation in expression of *EYA4* and one of its potential binding partners, *SIX1*. Expression profiles of *EYA1, EYA2, EYA4, and SIX1-4* genes show differential expression of multiple family members in more than one MPNST sample relative to normal Schwann cells. Expression of *PAX6* was also upregulated in all primary MPNSTs and 11 of 13 MPNST cell lines (Figure 1a), and PAX6 is transcriptionally upstream of SIX and EYA in the RD pathway. Furthermore, expression of *DACH1* was downregulated in MPNSTs (Figure 1a). Down-regulation of *DACH1* and up-regulation in *EYA1, EYA2, EYA4* and *SIX1-4*. *DACH1* expression is lower than normal in most benign neurofibroma samples as well as MPNST samples. Expression levels of *EYA4* and *SIX1* are statistically different (ANOVA; FDR = 0.01) between benign neurofibromas and MPNSTs and up-regulated at least three-fold in all MPNST samples (Figure 1a).

We confirmed the gene expression microarray data revealing differential expression of *PAX6, EYA, SIX1*, and *DACH1* in MPNSTs relative to NHSCs using quantitative real-time PCR (QRT-PCR) (Figure 1b – e). The magnitude of differential expression obtained using QRT-PCR was higher as compared to the microarray results yet displayed the same trend. The QRT-PCR data corroborated the most robust overexpression in *EYA4* (Figure 1 c), ranging from 50-fold to over 800-fold above NHSCs (13-fold to 67-fold for microarray data). The microarray expression data for *DACH1* was somewhat variable in NHSCs (ranging from −3.7 to 3.2-fold relative to the mean), and one MPNST cell line, YST1, displayed overexpression of *DACH1* (Figure 1a). QRT-PCR results validated the microarray data, confirming reduced *DACH1* expression in all MPNST cell lines, with the exception of YST1, relative to 3 independent NHSC samples (Figure 1d).

The NF1-GAP related domain (GRD) regulates expression of *DACH1* in MPNST cells

The NF1-GRD is the best characterized domain of NF1, converting activated Ras to its inactivated form. To observe transcriptional changes downstream of the NF1-GRD, we conducted gene expression microarray analysis on MPNST cells 32 hours after infection with an adenovirus encoding the NF1-GRD (relative to a GFP control) (Figure 2a). This timepoint was chosen because it represents a significant reduction in Ras-GTP yet is prior to cell death induced by exogenous expression of the NF1-GRD (data not shown). Forty-five genes were differentially expressed (≥3-fold) in the MPNST 8814 cell line in response to the NF1-GRD expression (data not shown), including *DACH1*. Three of six *DACH1* probe sets confirmed the decrease in expression in ST8814 MPNST cells relative to NHSCs that was not significantly changed by infection with a control adenoviral vector but increased significantly subsequent to infection with the NF1-GRD adenovirus. Failure to show this expression pattern with three *DACH1* probe sets was likely due to probe set unreliability; note that data in Figure 1 is shown with these unreliable probe sets removed as described

(Daimaru *et al.* 1985). Expression of *PAX, EYA*, and *SIX* genes was not significantly altered by the NF1-GRD (Figure 2a), but *DACH1* expression was increased to a level comparable to NHSCs (Figure 2b).

Importantly, we confirmed that MPNST cells infected with the NF1-GRD adenovirus have significant reductions in Ras-GTP and downstream phospho-MEK and phospho-ERK protein levels at the 32 hour time point (Figure 2c). In addition, the significant increase in *DACH1* expression by the NF1-GRD adenovirus was not observed with a GFP adenovirus control (Figure 2d). These results were confirmed by a time-course QRT-PCR analysis, showing a progressive increase in *DACH1* expression levels from 18 – 32 hours in MPNST cells infected with the NF1-GRD relative to the GFP control (Figure 2e).

Reducing EYA4 expression inhibits MPNST cell adhesion and migration

To study the functional role for EYA4 in MPNST tumorigenesis, we first validated the microarray and QRT-PCR data by confirming elevated levels of EYA4 protein in MPNST cell lines relative to NHSCs at the protein level by western blotting. Two bands were observed in MPNST cell lines, likely representing the products of *EYA4* transcript variant 1 and transcript variant 2 (Borsani *et al.* 1999), but not in NHSCs (Figure 3a).

To observe the effects of reducing *EYA4* expression in MPNST cells, S462TY MPNST cell lines stably expressing EYA4 shRNAs were created. We observed a marked decrease in *EYA4* expression at the RNA level, as quantified by real time PCR (Figure 3b), and at the protein (Figure 3c) level using four independent EYA4 shRNAs compared to the shRNA control. Similar results were obtained in two additional independent MPNST cell lines (data not shown). The extent of EYA4 knockdown varied from 2- to 9-fold and was stable, as the pattern of expression across clones was retained through several cell passages (passage 1 – passage 6).

To test the effect of reducing EYA4 on specific cellular mechanisms that regulate MPNST cell behavior, we conducted functional assays *in vitro*. The rounded appearance of cells expressing *EYA4* shRNA several hours after plating and the lower number of cells remaining on plates after 4 days (Figure 3d) suggested a defect in cell adhesion that was confirmed in a cell adhesion assay (Figure 3e). When *EYA4* expression was reduced in MPNST cells, a 60 – 95% reduction in migration was evident, and the extent of inhibition of migration correlated with extent of reduction in EYA4 expression (Figure 3f). Thus, MPNST cell adhesion and motility are dependent on EYA4.

Reducing EYA4 expression induces MPNST cell death by necrosis

An apparently slower growth rate was observed in culturing the MPNST-shEYA4 cells. A modest decrease in cell accumulation was evident, yet not significant, in a nine day MTS assay (data not shown). Further investigation by FACS analysis confirmed no significant change in cell proliferation, apoptosis, or cell cycle progression. (Figure 4a–f). BrdU incorporation was used to confirm similar rates of proliferation in MPNST-shEYA4 and MPNST-shControl cells (data not shown). A similar small percentage of apoptotic cells

were detected in both MPNST cells expressing shEYA4 and shControl (Figure 4g) as confirmed by analysis of DNA fragmentation (data not shown).

Because fewer cells were present in growth assays with undetectable differences in proliferation or apoptosis, we tested if cell death by necrosis might account for the decrease in cell number. Necrotic cell death is associated with morphological changes including cell shrinkage, cytosolic condensation, membrane morphology changes, loss of anchorage and finally, cellular degradation (Krysko *et al.* 2008). Evidence of cell death by necrosis was observed in live cultures of MPNST-shEYA4 cells by the robust uptake of propidium iodide due to extensive membrane damage. Only 4.3% of S462TY cells expressing a scramble shRNA were PI+, whereas 15.0% of cells expressing EYA4.7 were PI+ (Krysko *et al.* 2008). To validate this observation we conducted flow cytometry. By flow cytometry, induction of cell death generally results in a shift of low side light scatter population to higher side light scatter population (Dive *et al.* 1992; Weston *et al.* 1994; Waring *et al.* 1999). To prevent analysis confusions with possible artifacts from cell aggregates and debris in suspension, our analysis by flow cytometry focused on cell singlets from adherent cells. Despite performing the flow cytometry analysis in the adherent cell fraction, which is enriched in surviving cells, there was a ~10% increase in light side scatter mean channel in cells expressing shEYA4 (Figure 4h).

Reducing EYA4 expression inhibits MPNST formation *in vivo* in xenografts

To determine if EYA4 expression is critical for MPNST tumorigenesis, we tested the MPNST-shEYA4 cells in a mouse xenograft model using the S462TY cell line. By 60 days, MPNST cells expressing three independent EYA4 shRNAs displayed significant reduction in tumor volumes (Figure 5a – b). As in the *in vitro* cell migration studies above (Figure 3f), we observed a correlation with levels of EYA4 and effects on tumor size. Expression levels of *EYA4* in MPNST-shEYA4.5 and MPNST-shEYA4.7 were reduced greater than 6-fold, and these cells did not develop detectable tumors; expression levels of *EYA4* in MPNST-shEYA4.3 were reduced only 2-fold, and these cells developed small tumors by 60 days. Reduced expression of *EYA4* was maintained in the MPNST-shEYA4.3 tumors relative to control tumors, as confirmed by QRT-PCR (Figure 5c).

Histological analyses revealed significant areas of necrosis within the shEYA4-expressing tumors (Figure 5e, g). Similar degrees of proliferation and apoptosis in control and shEYA tumors were confirmed with Ki67 staining (Figure 5h, i) and TUNEL assay (Figure 5j, k), respectively. CD31 staining revealed similar vascularity (Figure 5l, m).

Discussion

Microarray gene expression analysis revealed differential expression of members of the RD transcriptional network, *PAX6*, *EYA4*, *SIX1*, and *DACH1*, in MPNSTs relative to normal human Schwann cells. The NF1-GRD induced *DACH1* expression, implicating Ras signaling in the decreased *DACH1* expression seen in MPNSTs. Expression of *EYA4* was dramatically upregulated in MPNST cells and primary tumors, and inhibition of *EYA4* expression using shRNA reduced MPNST cell adhesion and migration and induced cell necrosis. Furthermore, tumorigenesis was profoundly inhibited when MPNST cells stably

expressing shEYA4 RNA were injected into athymic nude mice, again correlating with necrosis. Our previous study (Miller et al., 2009) provided evidence that overexpression of *SOX9* is sufficient to induce *EYA4* expression. We propose a model in which overexpression of SOX9 and loss of NF1 functions independently lead to dysregulation of the EYA4-SIX1-DACH1 transcription in MPNST.

The most dramatic differential expression was observed for *EYA4*, which was robustly overexpressed in all but one MPNST cell line and all primary MPNSTs, suggesting it and/or its family members, may represent an MPNST oncogene. Its activity may be context-specific, given other reports implicating *EYA4* as a tumor suppressor gene in gastrointestinal tumors (Zou *et al.* 2005; Osborn *et al.* 2006). The expression pattern of *PAX6, SIX1, EYA4*, and *DACH1* in MPNST cells suggests a scenario whereby expression of multiple members of a potential transcriptional network is dysregulated in a manner that promotes tumorigenesis. High levels of *PAX6, EYA4*, and *SIX1* expression in combination with low levels of *DACH1* expression are consistent with previous studies supporting a tumor promoting role for PAX (Maris *et al.* 1997; Muratovska *et al.* 2003), EYA (Ramdas *et al.* 2001), and SIX (Christensen *et al.* 2008) family members, and a tumor suppressor role for DACH1 (Wu *et al.* 2006; Wu *et al.* 2008; Wu *et al.* 2009). However, the existence of a transcriptional network involving these genes has not been demonstrated here and has not been definitively identified in mammalian cells.

This study and our previous studies used expression differences between cultured Schwann cells and MPNST cells to identify genes relevant to tumorigenesis (Miller et al., 2006, 2009). Gene expression changes are induced by cell isolation and tissue culture, and can interfere with the identification of relevant genes. In spite of these potential problems, our approach is supported by i*n vivo* validation of the microarray data in solid tumors for EYA4, coupled with functional validation in xenografts for EYA4.

Replacement of the NF1-GRD in MPNST cells rescued *DACH1* expression but did not alter transcription of *EYA* or *SIX* at 18 – 32 hours, although we cannot exclude the possibility that at other time points or levels of GRD expression transcription of *EYA* or *SIX* might be changed. It is possible that a primary effect of loss of NF1 on *DACH1* secondarily affects transcription of the other members of the complex. Indeed, several lines of evidence support feedback activation of the network members on each other (O'Neill *et al.* 1994). Furthermore, while only some neurofibroma samples have elevated *SIX1* or *EYA4* expression, *DACH1* expression was low in many neurofibroma Schwann cell cultures and primary neurofibromas. Thus, our data support the idea that decreased *DACH1* expression is an early event downstream of NF1 loss.

EYA4 was up-regulated in NF1-related and in sporadic MPNST cell lines, although Ras-GTP is not elevated in the same sporadic MPNST cells (Mahller *et al.* 2006). In addition, *EYA4* expression was not affected by replacing the NF1-GRD in NF1-deficient MPNST cells, suggesting NF1-Ras signaling does not regulate *EYA4* expression. In Drosophila it has been shown that Ras signaling phosphorylates EYA proteins, increasing its transcriptional activity (Hsiao *et al.* 2001; Silver *et al.* 2003). Thus, post-transcriptional regulation of EYA4 by the NF1-Ras pathway warrants future investigation. The mechanism(s) underlying high

EYA4 expression in MPNST remain to be definitively determined but is likely to involve elevated SOX9 expression. *SOX9* expression is elevated in both NF1-related and sporadic MPNST cell lines, and increasing SOX9 in wild type Schwann cells is sufficient to increase *EYA4* mRNA expression, while decreasing *SOX9* mRNA levels in MPNST cells decreases *EYA4* expression (Miller and Jessen *et al.* 2009).

Our results provide several lines of evidence supporting a role for EYA4 in cell survival, specifically in inhibition of cell death by necrosis. Cell death is generally classified as either apoptosis or necrosis, a major distinction being the early breakdown of the plasma membrane in necrotic cells (Kroemer *et al.* 2009). Molecular mechanisms regulating necrosis are not well understood, however overactivation of poly (ADP-ribose) polymerase (PARP) in response to extensive DNA damage results in depletion of ATP which can convert apoptosis to necrosis (Ha *et al.* 1999). The absence of changes in proliferation and apoptosis along with an increase in propidium iodide uptake suggested that necrosis may be the cause of decreased cell numbers in MPNST cells with reduced EYA4 expression. Further investigation *in vitro* supported necrotic cell death as increased side scatter was observed in FACS analysis. In addition, tumors that developed in xenografts of MPNST cells with low levels of EYA4 showed significant areas of necrosis. In other systems, loss of EYA induces apoptosis (Cook *et al.* 2009), suggesting the mechanism of cell death resulting from decreased EYA may depend upon co-regulatory factors. Our data also support a role for EYA4 in MPNST cell adhesion and migration both of which are inhibited in response to reducing EYA4 expression. A reduction in cell adhesion can prompt anoikis, however, anoikis is usually associated with apoptosis rather than necrosis. Cellular changes downstream of EYA4, including cell adhesion, migration, and survival, may reflect the metastatic behavior of MPNSTs (Klymkowsky *et al.* 2009) and provoke further investigation.

We conclude that the NF1-Ras pathway can regulate expression of *DACH1*, directly or indirectly, and EYA4 expression controls adhesion, migration, and blocks necrosis in MPNST cells. Inhibition of EYA4 reduced tumorigenic properties of MPNST cells *in vitro* and resulted in MPNST cell death *ex vivo*, suggesting that developing therapeutics aimed at diminishing *EYA4* expression or *EYA4* transcriptional targets represents a strategy for killing MPNST cells.

Acknowledgements

Viral vectors were produced by the Viral Vector Core at the Translational Core Laboratories, Cincinnati Children's Hospital Research Foundation, Cincinnati, Ohio. We thank Yonatan Y. Mahller for assistance with the xenograft experiments.

Support: This study was supported by an award from the DAMD (DOD W81XWH-04-1-0273) to N.R. and an NINDS Translational Neuroscience Award K01-NS049191-01A1 to S.M..

References

Abdelhak S, Kalatzis V, Heilig R, Compain S, Samson D, Vincent C, et al. A human homologue of the Drosophila eyes absent gene underlies branchio-oto-renal (BOR) syndrome and identifies a novel gene family. Nat Genet. 1997; 15(2):157–164. [PubMed: 9020840]

Basu TN, Gutmann DH, Fletcher JA, Glover TW, Collins FS, Downward J. Aberrant regulation of ras proteins in malignant tumour cells from type 1 neurofibromatosis patients. Nature. 1992; 356(6371): 663–664. [PubMed: 1570011]

Behbakht K, Qamar L, Aldridge CS, Coletta RD, Davidson SA, Thorburn A, et al. Six1 overexpression in ovarian carcinoma causes resistance to TRAIL-mediated apoptosis and is associated with poor survival. Cancer Res. 2007; 67(7):3036–3042. [PubMed: 17409410]

Borsani G, DeGrandi A, Ballabio A, Bulfone A, Bernard L, Banfi S, et al. EYA4, a novel vertebrate gene related to Drosophila eyes absent. Hum Mol Genet. 1999; 8(1):11–23. [PubMed: 9887327]

Carli M, Ferrari A, Mattke A, Zanetti I, Casanova M, Bisogno G, et al. Pediatric malignant peripheral nerve sheath tumor: the Italian and German soft tissue sarcoma cooperative group. J Clin Oncol. 2005; 23(33):8422–8430. [PubMed: 16293873]

Carroll SL, Ratner N. How does the Schwann cell lineage form tumors in NF1? Glia. 2008; 56(14): 1590–1605. [PubMed: 18803326]

Casella GT, Bunge RP, Wood PM. Improved method for harvesting human Schwann cells from mature peripheral nerve and expansion in vitro. Glia. 1996; 17(4):327–338. [PubMed: 8856329]

Christensen KL, Patrick AN, McCoy EL, Ford HL. The six family of homeobox genes in development and cancer. Adv Cancer Res. 2008; 101:93–126. [PubMed: 19055944]

Coletta RD, Christensen KL, Micalizzi DS, Jedlicka P, Varella-Garcia M, Ford HL. Six1 overexpression in mammary cells induces genomic instability and is sufficient for malignant transformation. Cancer Res. 2008; 68(7):2204–2213. [PubMed: 18381426]

Cook PJ, Ju BG, Telese F, Wang X, Glass CK, Rosenfeld MG. Tyrosine dephosphorylation of H2AX modulates apoptosis and survival decisions. Nature. 2009; 458(7238):591–596. [PubMed: 19234442]

Daimaru Y, Hashimoto H, Enjoji M. Malignant peripheral nerve-sheath tumors (malignant schwannomas). An immunohistochemical study of 29 cases. Am J Surg Pathol. 1985; 9(6):434–444. [PubMed: 3937453]

DeClue JE, Papageorge AG, Fletcher JA, Diehl SR, Ratner N, Vass WC, et al. Abnormal regulation of mammalian $p21^{ras}$ contributes to malignant tumor growth in von Recklinghausen (Type 1) neurofibromatosis. Cell. 1992; 69:265–273. [PubMed: 1568246]

Dive C, Gregory CD, Phipps DJ, Evans DL, Milner AE, Wyllie AH. Analysis and discrimination of necrosis and apoptosis (programmed cell death) by multiparameter flow cytometry. Biochim Biophys Acta. 1992; 1133(3):275–285. [PubMed: 1737061]

Evans DG, Baser ME, McGaughran J, Sharif S, Howard E, Moran A. Malignant peripheral nerve sheath tumours in neurofibromatosis 1. J Med Genet. 2002; 39(5):311–314. [PubMed: 12011145]

Ferner RE, Gutmann DH. International consensus statement on malignant peripheral nerve sheath tumors in neurofibromatosis. Cancer Res. 2002; 62(5):1573–1577. [PubMed: 11894862]

Friedman JM, Birch PH. Type 1 neurofibromatosis: a descriptive analysis of the disorder in 1,728 patients. Am J Med Genet. 1997; 70(2):138–143. [PubMed: 9128932]

Ha HC, Snyder SH. Poly(ADP-ribose) polymerase is a mediator of necrotic cell death by ATP depletion. Proc Natl Acad Sci U S A. 1999; 96(24):13978–13982. [PubMed: 10570184]

He TC, Zhou S, da Costa LT, Yu J, Kinzler KW, Vogelstein B. A simplified system for generating recombinant adenoviruses. Proc Natl Acad Sci U S A. 1998; 95(5):2509–2514. [PubMed: 9482916]

Holtkamp N, Reuss DE, Atallah I, Kuban RJ, Hartmann C, Mautner VF, et al. Subclassification of nerve sheath tumors by gene expression profiling. Brain Pathol. 2004; 14(3):258–264. [PubMed: 15446580]

Hsiao FC, Williams A, Davies EL, Rebay I. Eyes absent mediates cross-talk between retinal determination genes and the receptor tyrosine kinase signaling pathway. Dev Cell. 2001; 1(1):51–61. [PubMed: 11703923]

Ikeda K, Watanabe Y, Ohto H, Kawakami K. Molecular interaction and synergistic activation of a promoter by Six, Eya, and Dach proteins mediated through CREB binding protein. Mol Cell Biol. 2002; 22(19):6759–6766. [PubMed: 12215533]

Ismat FA, Xu J, Lu MM, Epstein JA. The neurofibromin GAP-related domain rescues endothelial but not neural crest development in Nf1 mice. J Clin Invest. 2006; 116(9):2378–2384. [PubMed: 16906226]

Josephson R, Muller T, Pickel J, Okabe S, Reynolds K, Turner PA, et al. POU transciption factors control expression of CNS stem cell-specific genes. Development. 1998; 125(16):3087–3100. [PubMed: 9671582]

Kim HA, Rosenbaum T, Marchionni MA, Ratner N, DeClue JE. Schwann cells from neurofibromin deficient mice exhibit activation of $p21^{ras}$, inhibition of cell proliferation and morphological changes. Oncogene. 1995; 11:325–335. [PubMed: 7624147]

Klose A, Robinson N, Gewies A, Kluwe L, Kaufmann D, Buske A, et al. Two novel mutations in exons 19a and 20 and a BsaBI [correction of BsaI] polymorphism in a newly characterized intron of the neurofibromatosis type 1 gene. Hum Genet. 1998; 102(3):367–371. [PubMed: 9544853]

Klymkowsky MW, Savagner P. Epithelial-mesenchymal transition: a cancer researcher's conceptual friend and foe. Am J Pathol. 2009; 174(5):1588–1593. [PubMed: 19342369]

Kobayashi M, Nishikawa K, Suzuki T, Yamamoto M. The homeobox protein Six3 interacts with the Groucho corepressor and acts as a transcriptional repressor in eye and forebrain formation. Dev Biol. 2001; 232(2):315–326. [PubMed: 11401394]

Kroemer G, Galluzzi L, Vandenabeele P, Abrams J, Alnemri ES, Baehrecke EH, et al. Classification of cell death: recommendations of the Nomenclature Committee on Cell Death 2009. Cell Death Differ. 2009; 16(1):3–11. [PubMed: 18846107]

Krysko DV, Vanden Berghe T, Parthoens E, D'Herde K, Vandenabeele P. Methods for distinguishing apoptotic from necrotic cells and measuring their clearance. Methods Enzymol. 2008; 442:307–341. [PubMed: 18662577]

Leroy K, Dumas V, Martin-Garcia N, Falzone M-C, Voisin M-C, Wechsler J, et al. Malignant peripheral nerve sheath tumors associated with neurofibromatosis type 1. Arch Dermatol. 2001; 137:908–913. [PubMed: 11453810]

Li X, Oghi KA, Zhang J, Krones A, Bush KT, Glass CK, et al. Eya protein phosphatase activity regulates Six1-Dach-Eya transcriptional effects in mammalian organogenesis. Nature. 2003; 426(6964):247–254. [PubMed: 14628042]

Mahller YY, Rangwala F, Ratner N, Cripe TP. Malignant peripheral nerve sheath tumors with high and low Ras-GTP are permissive for oncolytic herpes simplex virus mutants. Pediatr Blood Cancer. 2006; 46(7):745–754. [PubMed: 16124003]

Mahller YY, Vaikunth SS, Currier MA, Miller SJ, Ripberger MC, Hsu YH, et al. Oncolytic HSV and erlotinib inhibit tumor growth and angiogenesis in a novel malignant peripheral nerve sheath tumor xenograft model. Mol Ther. 2007; 15(2):279–286. [PubMed: 17235305]

Mahller YY, Vaikunth SS, Ripberger MC, Baird WH, Saeki Y, Cancelas JA, et al. Tissue inhibitor of metalloproteinase-3 via oncolytic herpesvirus inhibits tumor growth and vascular progenitors. Cancer Res. 2008; 68(4):1170–1179. [PubMed: 18281493]

Maris JM, Wiersma SR, Mahgoub N, Thompson P, Geyer RJ, Hurwitz CG, et al. Monosomy 7 myelodysplastic syndrome and other second malignant neoplasms in children with neurofibromatosis type 1. Cancer. 1997; 79(7):1438–1446. [PubMed: 9083167]

McCormick F. Ras signaling and NF1. Curr Opin Genet Dev. 1995; 5(1):51–55. [PubMed: 7749326]

Miller SJ, Rangwala F, Williams J, Ackerman P, Kong S, Jegga AG, et al. Large-scale molecular comparison of human schwann cells to malignant peripheral nerve sheath tumor cell lines and tissues. Cancer Res. 2006; 66:2584–2591. [PubMed: 16510576]

Muratovska A, Zhou C, He S, Goodyer P, Eccles MR. Paired-Box genes are frequently expressed in cancer and often required for cancer cell survival. Oncogene. 2003; 22(39):7989–7997. [PubMed: 12970747]

Ng KT, Man K, Sun CK, Lee TK, Poon RT, Lo CM, et al. Clinicopathological significance of homeoprotein Six1 in hepatocellular carcinoma. Br J Cancer. 2006; 95(8):1050–1055. [PubMed: 17008870]

O'Neill EM, Rebay I, Tjian R, Rubin G. The activities of two Ets related transcription factors required for Drosophila eye development are modulated by the Ras/MAPK pathway. Cell. 1994; 78:137–147. [PubMed: 8033205]

Osborn NK, Zou H, Molina JR, Lesche R, Lewin J, Lofton-Day C, et al. Aberrant methylation of the eyes absent 4 gene in ulcerative colitis-associated dysplasia. Clin Gastroenterol Hepatol. 2006; 4(2):212–218. [PubMed: 16469682]

Ramdas L, Coombes KR, Baggerly K, Abruzzo L, Highsmith WE, Krogman T, et al. Sources of nonlinearity in cDNA microarray expression measurements. Genome Biology. 2001; 2(11):1–7.

Rasmussen SA, Friedman JM. NF1 gene and neurofibromatosis 1. Am J Epidemiol. 2000; 151(1):33–40. [PubMed: 10625171]

Rayapureddi JP, Kattamuri C, Steinmetz BD, Frankfort BJ, Ostrin EJ, Mardon G, et al. Eyes absent represents a class of protein tyrosine phosphatases. Nature. 2003; 426(6964):295–298. [PubMed: 14628052]

Reichenberger KJ, Coletta RD, Schulte AP, Varella-Garcia M, Ford HL. Gene amplification is a mechanism of Six1 overexpression in breast cancer. Cancer Res. 2005; 65(7):2668–2675. [PubMed: 15805264]

Serra E, Rosenbaum T, Winner U, Aledo R, Ars E, Estivill X, et al. Schwann cells harbor the somatic *NF1* mutation in neurofibromas: evidence of two different Schwann cell populations. Human Molecular Genetics. 2000; 9(20):3055–3064. [PubMed: 11115850]

Sherman LS, Atit R, Rosenbaum T, Cox AD, Ratner N. Single cell Ras-GTP analysis reveals altered Ras activity in a subpopulation of neurofibroma Schwann cells but not fibroblasts. Journal of Biological Chemistry. 2000; 275(39):30740–30745. [PubMed: 10900196]

Silver SJ, Davies EL, Doyon L, Rebay I. Functional dissection of eyes absent reveals new modes of regulation within the retinal determination gene network. Mol Cell Biol. 2003; 23(17):5989–5999. [PubMed: 12917324]

Silver SJ, Rebay I. Signaling circuitries in development: insights from the retinal determination gene network. Development. 2005; 132(1):3–13. [PubMed: 15590745]

Tootle TL, Silver SJ, Davies EL, Newman V, Latek RR, Mills IA, et al. The transcription factor Eyes absent is a protein tyrosine phosphatase. Nature. 2003; 426(6964):299–302. [PubMed: 14628053]

Viskochil D, Carey JC. Nosological considerations of the neurofibromatoses. J Dermatol. 1992; 19(11):873–880. [PubMed: 1293176]

Vogel KS, Klesse LJ, Velasco-Miguel S, Meyers K, Rushing EJ, Parada LF. Mouse tumor model for neurofibromatosis type 1. Science. 1999; 286:2176–2179. [PubMed: 10591653]

Waring P, Lambert D, Sjaarda A, Hurne A, Beaver J. Increased cell surface exposure of phosphatidylserine on propidium iodide negative thymocytes undergoing death by necrosis. Cell Death Differ. 1999; 6(7):624–637. [PubMed: 10453073]

Watson MA, Perry A, Tihan T, Prayson RA, Guha A, Bridge J, et al. Gene expression profiling reveals unique molecular subtypes of Neurofibromatosis Type I-associated and sporadic malignant peripheral nerve sheath tumors. Brain Pathol. 2004; 14(3):297–303. [PubMed: 15446585]

Weston KM, Alsalami M, Raison RL. Cell membrane changes induced by the cytolytic peptide, melittin, are detectable by 90 degrees laser scatter. Cytometry. 1994; 15(2):141–147. [PubMed: 8168400]

Wu K, Katiyar S, Li A, Liu M, Ju X, Popov VM, et al. Dachshund inhibits oncogene-induced breast cancer cellular migration and invasion through suppression of interleukin-8. Proc Natl Acad Sci U S A. 2008; 105(19):6924–6929. [PubMed: 18467491]

Wu K, Katiyar S, Witkiewicz A, Li A, McCue P, Song LN, et al. The cell fate determination factor dachshund inhibits androgen receptor signaling and prostate cancer cellular growth. Cancer Res. 2009; 69(8):3347–3355. [PubMed: 19351840]

Wu K, Li A, Rao M, Liu M, Dailey V, Yang Y, et al. DACH1 is a cell fate determination factor that inhibits cyclin D1 and breast tumor growth. Mol Cell Biol. 2006; 26(19):7116–7129. [PubMed: 16980615]

Xu LZ, Sanchez R, Sali A, Heintz N. Ligand specificty of brain lipid-binding protein. Journal of Biological Chemistry. 1996; 271(40):24711–24719. [PubMed: 8798739]

Zhu CC, Dyer MA, Uchikawa M, Kondoh H, Lagutin OV, Oliver G. Six3-mediated auto repression and eye development requires its interaction with members of the Groucho-related family of co-repressors. Development. 2002; 129(12):2835–2849. [PubMed: 12050133]

Zou H, Osborn NK, Harrington JJ, Klatt KK, Molina JR, Burgart LJ, et al. Frequent methylation of eyes absent 4 gene in Barrett's esophagus and esophageal adenocarcinoma. Cancer Epidemiol Biomarkers Prev. 2005; 14(4):830–834. [PubMed: 15824152]

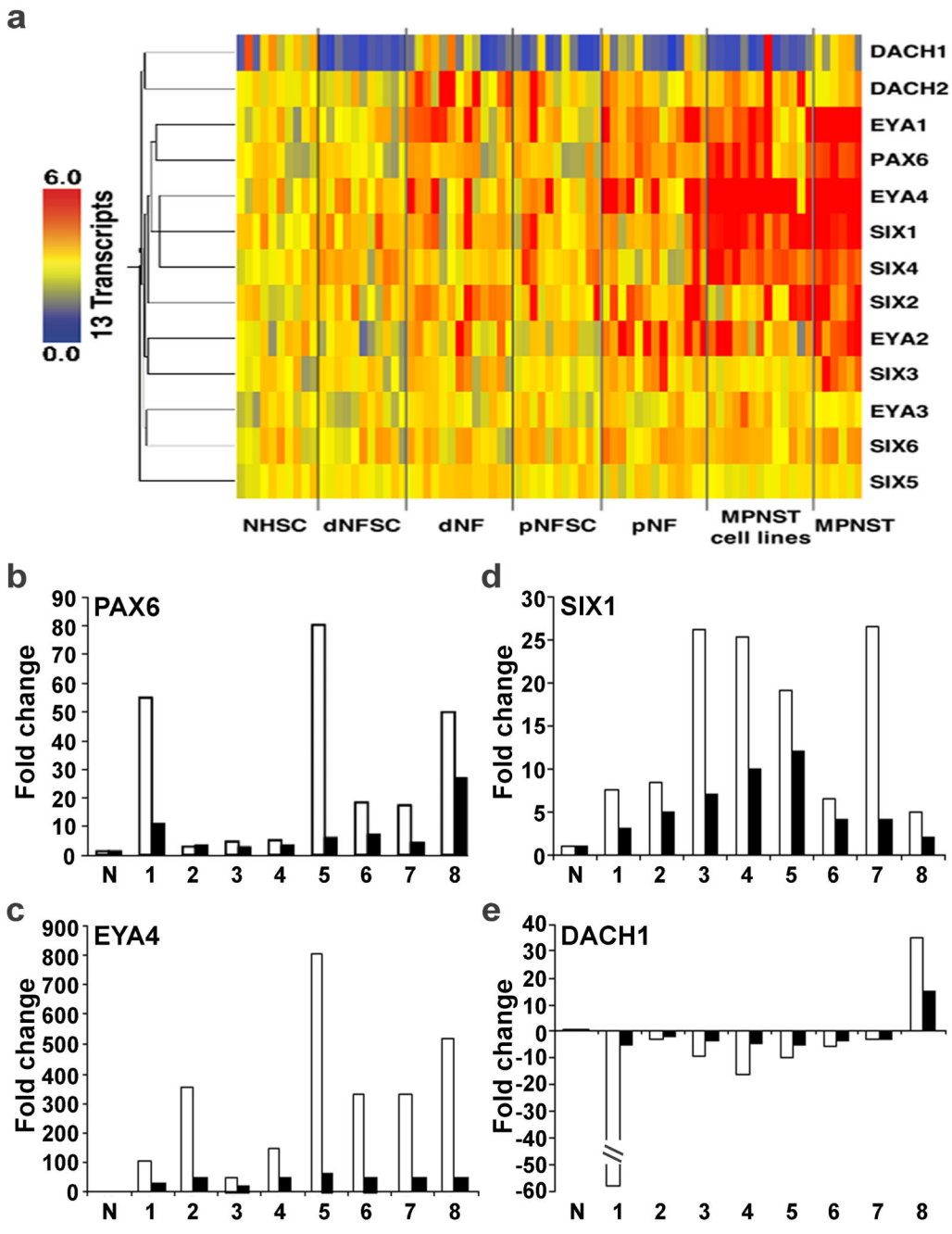

Figure 1. Expression of the PAX/EYA/SIX/DACH transcriptional complex is dysregulated in MPNST

(a) Hierarchical clustering of gene expression microarray data of *PAX*, *EYA*, *SIX*, *and DACH* genes family members. *EYA4*, *SIX1*, and *PAX6* expression in MPNST are statistically (ANOVA; FDR=.01) different from normal Schwann cells or neurofibroma samples. MPNST samples expressed, on average, at least three-fold higher levels of each mRNA relative to neurofibroma samples or normal Scwann cells. MPNST samples (n=6 primary MPNSTs; n=13 MPNST cell lines). Yellow = normal; Red = overexpression; Blue =

underexpression. *DACH1* expression is down-regulated in MPNST cell lines and the majority of benign neurofibroma samples. (b) Confirmation of microarray gene expression data for *PAX6*, *SIX1*, *EYA4*, and *DACH1* using quantitative real time PCR (QRT-PCR). Black bars = microarray data; White bars = QRT-PCR data. QRT-PCR values shown are fold-change in expression relative to normal human Schwann cells (N). Samples 1 – 8 are MPNST cell lines: 1 = STS26T; 2 = ST8814; 3 = S462; 4 = T265; 5 = S520; 6 = 90-8; 7 = 88-3; 8 = YST1.

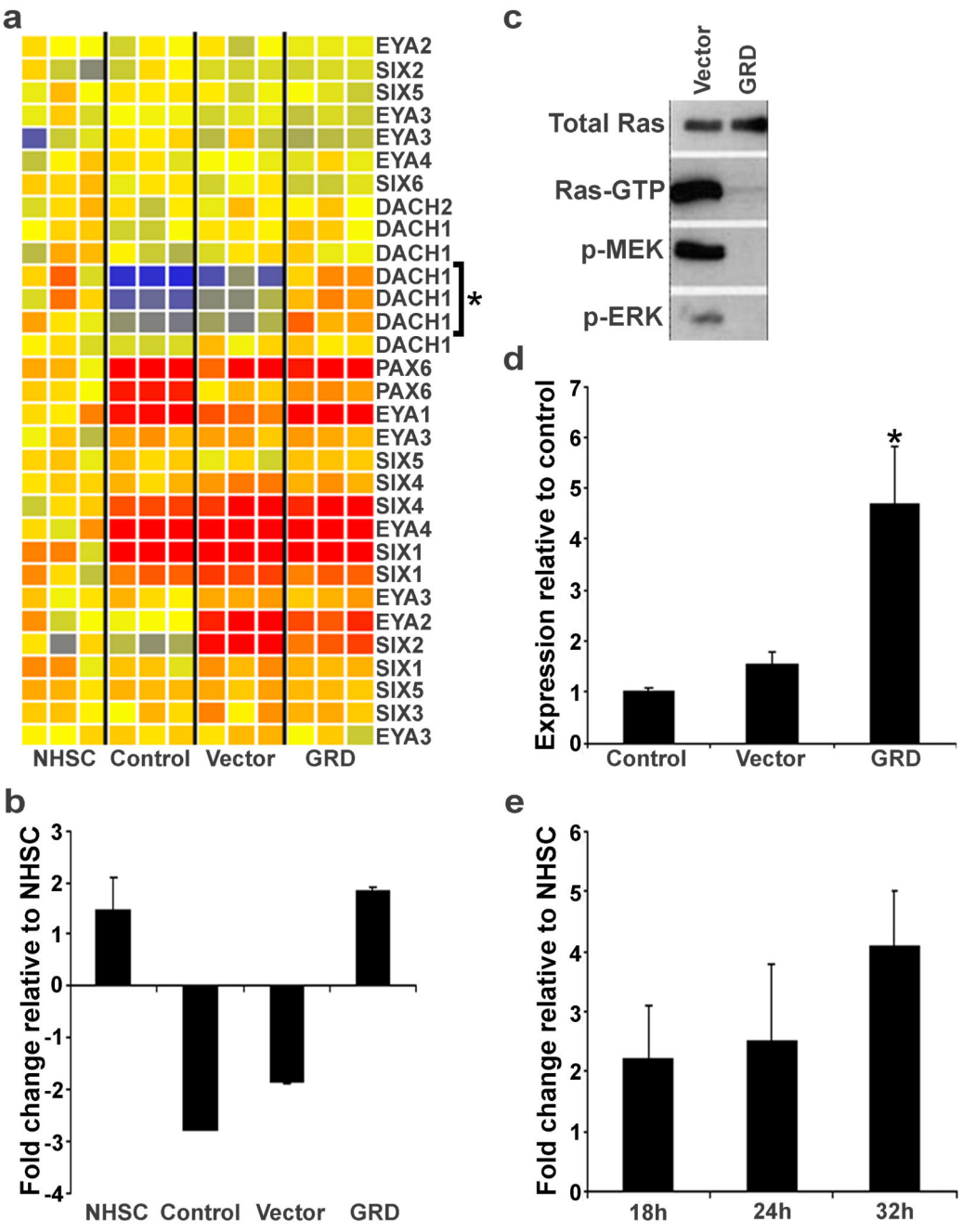

Figure 2. The NF1-GRD normalizes *DACH1* expression

(a) Gene expression microarray data of normal human Schwann cells (NHSC), and ST8814 NF1 patient-derived MPNST cells (control) infected with an adenoviral vector expressing GFP (Vector) or the NF1-GRD (GRD). Samples were analyzed in triplicate, and expression is shown relative to the mean of the NHSC samples. Yellow = normal; Red = overexpression; Blue = underexpression. (b) The microarray expression data for the three DACH1 probesets designated by the * in (a) is expressed as fold-change relative to NHSC, showing normalization of *DACH1* expression by the NF1-GRD. (c) The NF1-GRD

adenovirus blocks Ras/Map-kinase signaling in ST8814 MPNST cells. Ras-GTP was measured in cell lysates after control (Vector) or GRD infection. Ras-GTP, phospo-MEK and phospho-ERK protein levels were each diminished in the presence of the NF1-GRD. (d) Quantification of NF1-GRD effects on *DACH1* expression in ST8814 MPNST cells in the gene expression microarray. (e) Confirmation of increased levels of *DACH1* expression in response to the NF1-GRD at 18, 24, and 32 hours post-infection using QRT-PCR. Values are fold-change in expression relative to adenoviral vector control.

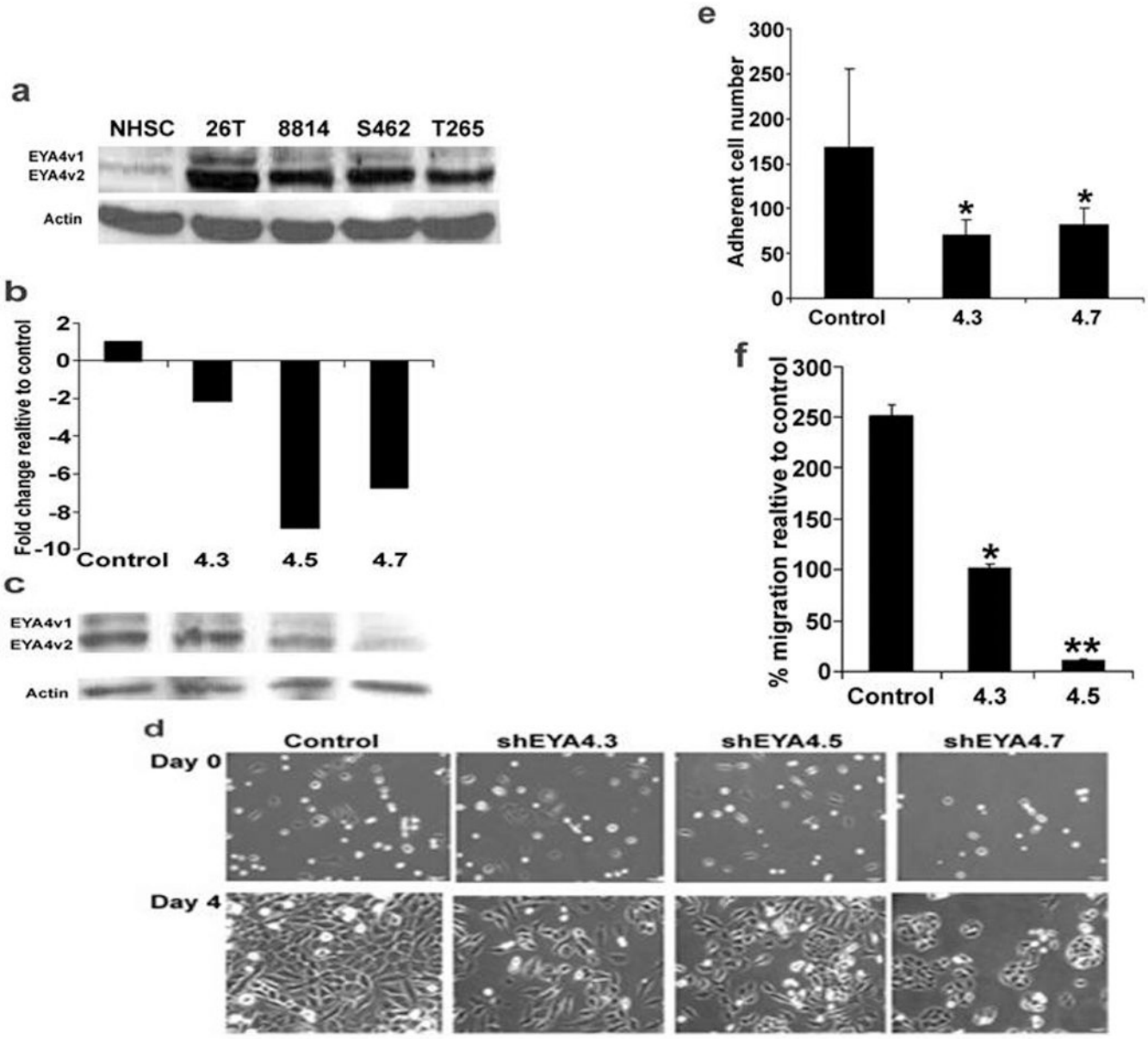

Figure 3. Reducing EYA4 expression with shRNA inhibits cell adhesion and migration

(a) EYA4 protein is expressed in MPNST cell lines (STS26T, ST8814, S462, T265) but not normal human Schwann cells (NHSC), assessed by western blotting. Staining with anti-actin confirmed equal amounts of protein across samples. (b, c) EYA4 expression in S462TY MPNST cells is reduced subsequent to introduction of shEYA4 RNAs (4.3, 4.4, 4.5, 4.7). Data are shown for level of RNA using QRT-PCR (b) and protein by western blotting with anti-EYA4 or an anti-AKT loading control (c). (d) Phase contrast micrographs of living S462TY cells at day 0 (d0) and day 4 (d4). Fewer S462TY cells containing shEYA4 shRNAs attach to dishes, correlating with decreased cell numbers at day 4. (e) Adhesion assay of S462TY cells containing control or shEYA4 cells. Significantly fewer cells remain attached (*$p<0.05$) in the presence of EYA4 shRNAs (4.3, 4.7) relative to control shRNA.

(f) Migration of S462TY MPNST cells through transwell filters is significantly reduced (*$p<0.05$; **$p<0.01$) in the presence of EYA4 shRNAs (4.3, 4.4, 4.5). Values are expressed as percent migration relative to control shRNA.

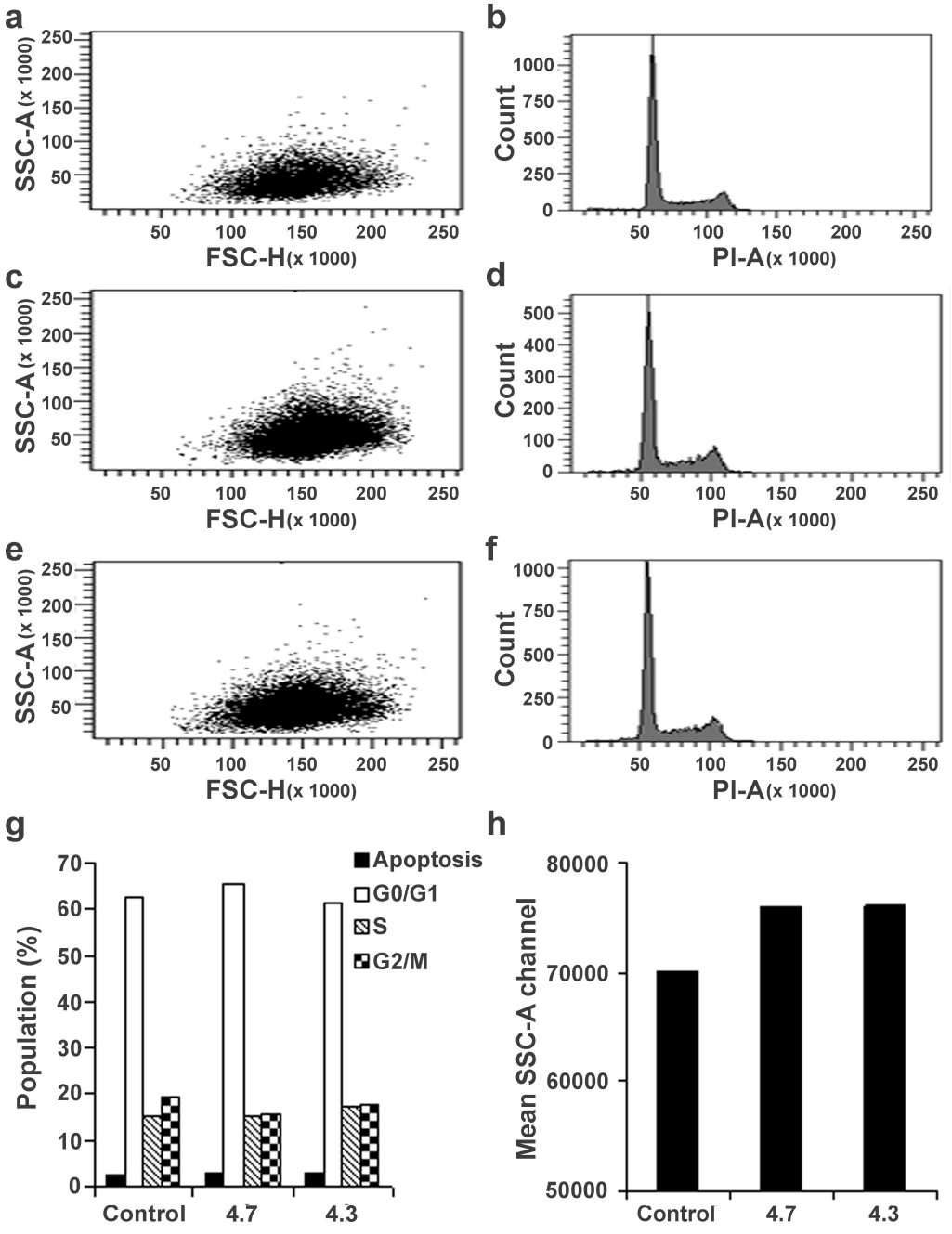

Figure 4. Reducing EYA4 expression causes MPNST cell death by necrosis

shControl (a, b), MPNST-shEYA4.7 (c, d), or MPNST-shEYA4.3 (e,f) cells were fixed and stained with propidium iodide. Flow cytometry analysis of forward scatter (FSC) and side scatter (SSC) in linear amplification was performed along cell cycle analysis are shown in a, c, and e. Identification of the A_o (apoptotic), G_o/G, S, and G2/M peaks are shown in b, d, and f. (g) Quantification of cell cycle shows no differences in control or shEYA4.7 or 4.3 cells. (h) A 10% increase in light side scatter mean channel is shown in cells expressing shEYA44.3 or 4.7 as compared to control.

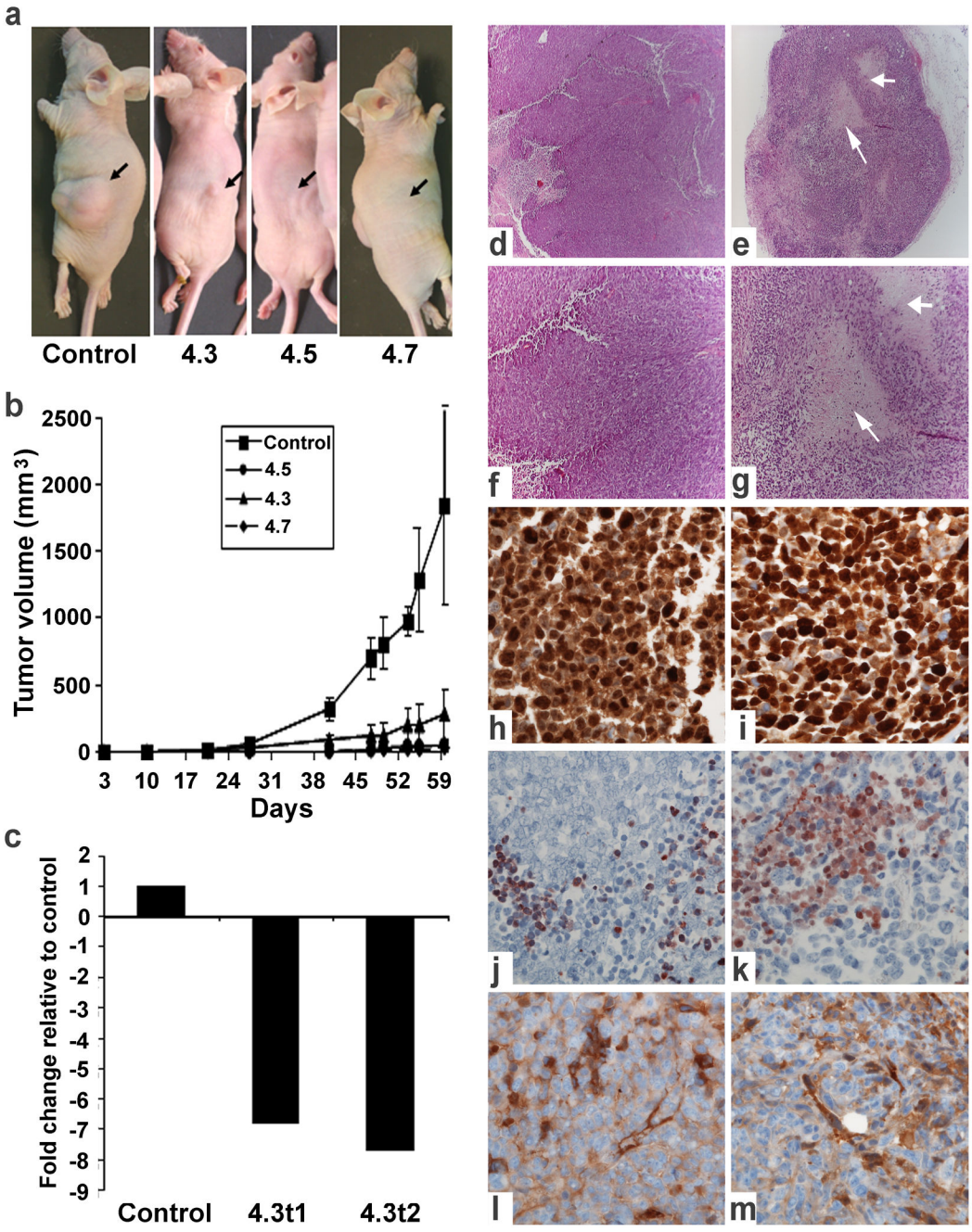

Figure 5. Reducing EYA4 expression inhibits tumorigenesis

(a) Gross photographs of nude mice tumors. Black arrows point to flank tumors in mice injected with MPNST cells expressing sh-scramble or shEYA4.3, 4.5, or 4.7. (b) Quantification of tumor volume over time. (c) QRT-PCR showing persistent EYA4 downregulation in small tumors dissected from two mice 59 days after implantation with shEYA44.3, to control for possible loss of shEYA4 expression. (d, f, h, j, l) are photomicrographs of control, and (e, g, i, k, m) are of shEya4.3 tumors (d,e) Low power views of hematoxylin-eosin stain of control (d) tumor and the smaller shEya (e) tumors

(40×). The shEya tumor exhibits disproportionate necrosis. (f, g) Higher power views of each tumor. Larger amounts of necrosis in shEya tumor (f) compared to control (scramble) tumor (g) is apparent (100×). Ki67 stains of control (h) and shEya (i) tumors exhibiting similar degree of proliferation. (400×). Tunel assay of control (j) and shEya (k) tumors exhibiting similar degrees of apoptosis (400×). CD31 stain of control (l) and ShEya (m) tumors exhibiting similar vascularity (400×).